



High-energy high-efficiency Nd:YLF laser end-pump by 808 nm diode

Qinglei Ma ^{*}, Haiding Mo, Jay Zhao

Advanced Optowave Corporation, 105 Comac St, Ronkonkoma, NY 11779, United States

ARTICLE INFO

Keywords:

Diode-pumped laser
Laser resonator
Q-switched
Nd:YLF

ABSTRACT

A model is developed to calculate the optimal pump position for end-pump configuration. The 808 nm wing pump is employed to spread the absorption inside the crystal. By the optimal laser cavity design, a high-energy high-efficiency Nd:YLF laser operating at 1053 nm is presented. In cw operation, a 13.6 W power is obtained with a slope efficiency of 51% with respect to 30 W incident pump power. The beam quality is near diffraction limited with $M^2 \sim 1.02$. In Q-switch operation, a pulse energy of 5 mJ is achieved with a peak power of 125 kW at 1 kHz repetition rate.

© 2017 Elsevier B.V. All rights reserved.

1. Introduction

Diode-pumped-solid-state (DPSS) lasers have attracted considerable attention in recent years. [1–4] Their wide applications have stepped into various areas, such as material processing, medical treatment, etc. [5,6] Among the Nd-based DPSS lasers, Nd:YLF lasers are of special interest, especially in high energy Q-switched lasers operating at low repetition rates. The uniaxial Nd:YLF crystal is of natural birefringence, which overwhelms thermally induced birefringence eliminating the thermal depolarization problem of isotropic crystals like Nd:YAG. [7,8] Moreover, its longer fluorescence lifetime ($\sim 480 \mu\text{s}$), offering higher capability of energy storage, make it more competitive in high energy pulse lasers compared with Nd:YAG ($\sim 230 \mu\text{s}$) and Nd:YVO₄ ($\sim 100 \mu\text{s}$) crystals. In addition, Nd:YLF operating at 1053 nm corresponding to σ polarization exists weak thermal lensing effect because the negative temperature dependence of the refractive index partially compensates the positive temperature dependence of thermal expansion coefficient. [9,10] The net result is that the power of the thermal lens in Nd:YLF is typically a factor of 17 smaller than in Nd:YAG under comparable pumping conditions. [11] The relatively low thermal lensing effect which typically coincides with reduced thermal aberrations makes it possible to generate near diffraction-limited beam quality.

End-pumped Nd:YLF lasers have been widely studied because the end pumping configuration has the advantage of excellent mode match, leading to good beam quality and high conversion efficiency. [12–15] The pump optimization for end-pumped configuration has been studied for a long time. [16–18] However, there is no effective pump model reported to investigate the optimal end-pump position, so as to improve laser output performance. Most of the previous works were talking about

only the mode-match to improve the overlap efficiency so as to improve the conversion efficiency. However, based on our experience, the pump position is also crucial to the laser efficiency in addition to the mode match. For end-pump structure it exists an optimal pumping position where the maximum output is achieved. If the pump position is not at the optimal point, the output is always relatively lower no matter how good the mode match is achieved. Besides, though the weak thermal lensing effect of Nd:YLF seems to be a benefit to its power scaling, the Nd:YLF crystal has a tendency to fracture under high pump density. The fracture limit for Nd:YLF is ~ 5 times lower than that for Nd:YAG. [19] In end-pumped Nd:YLF lasers, the pump power is incident into crystals from a small volume, which makes it easier to fracture. Therefore, reducing the stressed fracture should be considered in the cavity design of end-pumped Nd:YLF lasers.

In this paper, we firstly build up a model to investigate the total gain inside the crystal with different pump positions. Through this model, the optimal position is determined, at which the Nd:YLF obtains the largest gain from pump. In order to decrease the stressed fracture of Nd:YLF crystal, the wavelength at absorption peak $\sim 797 \text{ nm}$ is not used. On the contrary, a low absorption coefficient of 808 nm is employed as the pump, which is typically called ‘wing pump’. Besides, a relatively longer but lower Nd-doped (0.5%) crystal is used to spread the absorption. Both the wing pump scheme and low Nd-doped crystal reduce the up-conversion and spread out the absorption and thermal load longitudinally in the crystal, increasing the thermal fracture pump limit. Moreover, in order to achieve near diffraction-limited beam quality and high conversion efficiency, the laser cavity is precisely designed for good mode match. Eventually, a 13.5 W 1053 nm Nd:YLF

^{*} Corresponding author.

E-mail address: qingleima@yeah.net (Q. Ma).

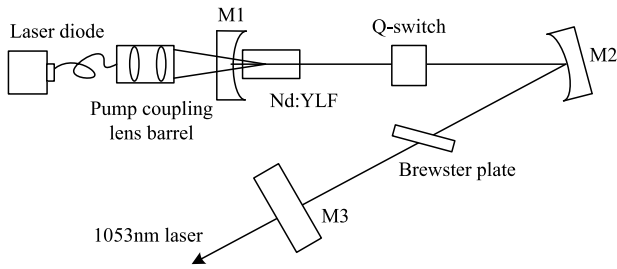


Fig. 1. Schematic diagram of Nd:YLF laser.

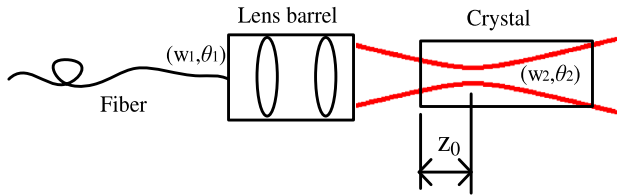


Fig. 2. Scheme of pump structure.

laser with near-diffraction-limited beam ($M^2 = 1.02$) is obtained under continuous wave (cw) operation at 30 W 808 nm pump. The optical to optical efficiency and slope efficiency with respect to the incident pump power are $\sim 45\%$ and $\sim 51\%$, respectively. Under the Q-switch operation, a high pulse energy of 5 mJ is obtained at 1 kHz repetition rate.

2. Experimental setup

2.1. Setup of Nd:YLF laser

The experimental configuration of Nd:YLF laser is shown in Fig. 1. A simple folded cavity structure is employed consisting three mirrors. The cavity length is 720 mm. M1 is the pump mirror with a curvature of $R = 500$ mm, coated with high reflection at 1053 nm and anti-reflection at 808 nm. M2 has a curvature of $R = 400$ mm with high reflection at 1053 nm. M3 is the output coupler of 1053 nm laser. Under the cw operation, $T = 15\%$ is employed to achieve optimal output. But in Q-switch operation at 1 kHz, $T = 35\%$ is used in order to avoid damaging dielectric coatings from high peak power laser pulse. The 0.5% doped Nd:YLF crystal (CASTECH Inc) is 3 mm-diameter by 35 mm-length. The Nd:YLF is a-axis-cut, and its optical axis is perpendicular to the plane of optical table. The two end-faces of rod were with anti-reflective coating at 1053 nm and 808 nm. The Nd:YLF rod is wrapped with Indium foil and mounted on a water cooled copper block. An acousto-optical Q switch with AR coating at 1053 nm is employed for 1 kHz pulse operation. A Brewster plate is inserted into the cavity to suppress the oscillation of 1047 nm laser line and ensure that only the 1053 nm laser line oscillates throughout the whole pumping process. The Nd:YLF rod is pumped by a 0.22 N.A. fiber coupled 808 nm laser diode with a maximum power of 30 W. The 808 nm diode laser is focused into the Nd:YLF rod at a spot size diameter of ~ 0.96 mm after a pumping coupling lens barrel system.

2.2. Optimal pump position

The diode laser is focused into the rod after the lens barrel system, as is shown in Fig. 2. The spot size diameter at focal point is measured to be 0.96 mm. The total gain of pump varies when the focal point is at different positions giving various pumping volume inside the crystal. The optimal pump position z_0 can be determined where the pumping laser generates the maximum gain inside the crystal rod.

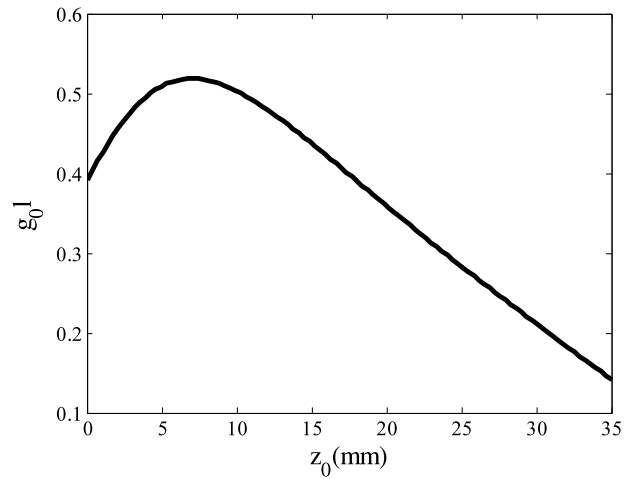


Fig. 3. Small signal gain as a function of position z_0 .

At the end of fiber before the lens barrel coupling system, the beam waist and divergent angle is w_1 and θ_1 , satisfying:

$$w_1 \theta_1 = M^2 \frac{\lambda}{\pi}, \quad (1)$$

where w_1 equals the radius of fiber core 200 μm and θ_1 is the N.A. of fiber (0.22). λ is the pump wavelength. Then, the beam quality factor M^2 is calculated to be 170. After the lens barrel, the pump beam propagation is described as:

$$w(z) = w_2 \sqrt{1 + \left(\frac{z}{z_R}\right)^2}, \quad (2)$$

where $z_R = \frac{n\pi w_2^2}{\lambda M^2}$ is the Rayleigh length and w_2 is 0.48 mm. The refractive index n of Nd:YLF crystal is 1.45. And the z_R is calculated to be ~ 8 mm. Since the beam quality factor M^2 of diode laser is very large, we treat the beam as flat-top. At the pump position of z_0 the total gain generated from pump laser inside the rod is expressed as [20]:

$$g_0 I(z_0) = \int_{-z_0}^{d-z_0} \frac{\eta_s p \alpha \exp(-\alpha(z+z_0))}{I_s \pi w^2(z)} dz, \quad (3)$$

where d is the crystal length, η_s is Stokes efficiency, p is the pump power, and I_s is the saturation density. Absorption coefficient α of the Nd:YLF crystal is measured to be 0.06 mm^{-1} . The simulation result is presented in Fig. 3. It shows that the maximum gain occurs at $z_0 = \sim 7$ mm. Hence in our experiment, we set the beam waist of pump laser 7 mm inside the crystal.

2.3. Beam mode

Good mode matching between the pump profile and laser profile enhances the optical conversion and improve the beam quality. Though the thermal lensing is weak in the Nd:YLF crystal, it is still necessary to design a broad stable resonator. By using the ABCD matrix and mode self-consistency condition, [21,22] the beam size distribution in the cavity can be simulated. Fig. 4 shows the beam mode sizes at the crystal under different thermal focal lengths. It can be seen that the resonator is designed with a stable cavity under broad thermal focal length range. Besides, the beam mode size maintains nearly a constant throughout a wide range of thermal focal length, indicating a good beam mode matching throughout the whole pump power range.

3. Results and discussion

Both cw and pulse output performances are studied in this work. Fig. 5 shows the cw output power as a function of incident 808 nm

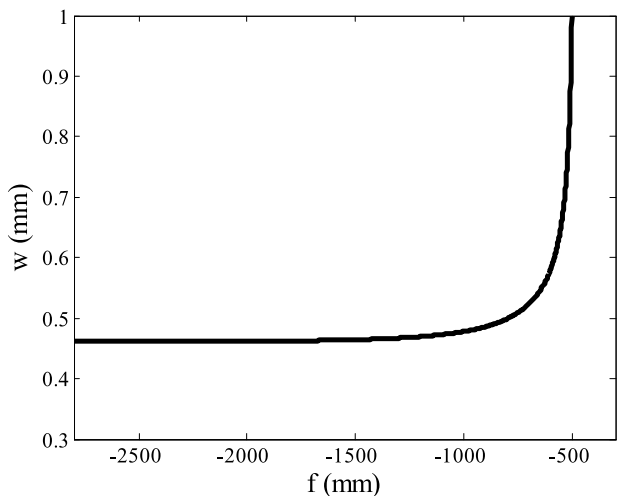


Fig. 4. Beam mode size versus thermal focal length.

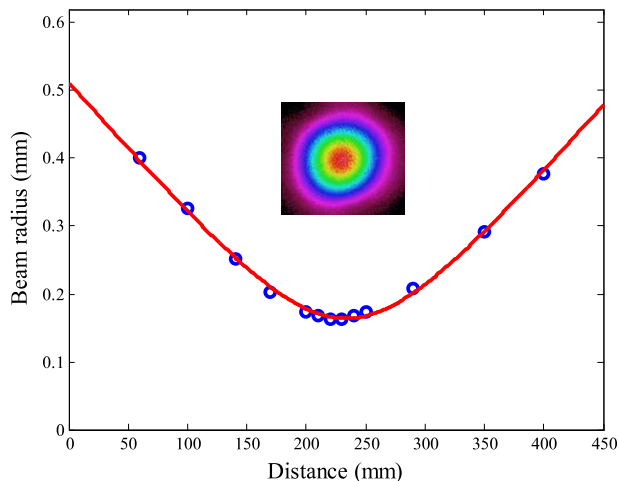


Fig. 6. Beam quality factor M^2 measurement of 1053 nm laser.

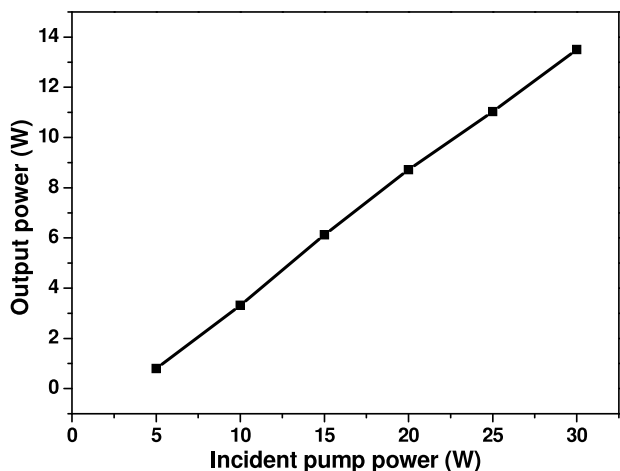


Fig. 5. Output power of cw operation versus incident 808 nm pump power.

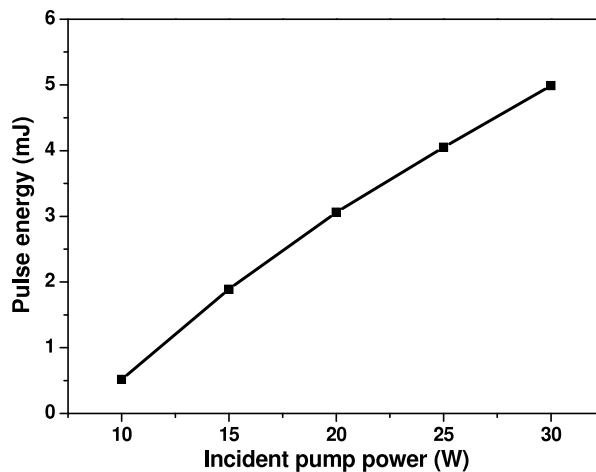


Fig. 7. Pulse energy at 1 kHz repetition rate versus incident pump power.

pump power. The threshold occurs at ~ 2 W pump power. At maximum pump power of 30 W, the 1053 nm laser output power is 13.5 W, corresponding to an optical-to-optical efficiency of 45%. The average slope efficiency is 51% with respect to the incident pump power. The Nd:YLF crystal offers an absorption efficiency of 90% of 808 nm power, implying that the conversion efficiencies should be 10% higher with respect to the absorbed power. Besides, the output power linearly increases with pump power. Higher output power is expected when using larger power 808 nm diode.

The output beam is relatively elliptical at the maximum output. A cylindrical lens is inserted in front of the crystal to correct the beam profile. Finally, a roundness of 99% beam profile is obtained. The beam quality factor M^2 is also measured with the aid of CCD, as is shown in Fig. 6. The M^2 is measured to be ~ 1.02 implying a near diffraction limited beam is obtained.

Nd:YLF is much attractive in high energy pulse lasers at low repetition rates. In this work, the Q-switched laser performance at 1 kHz repetition rate is studied. Fig. 7 shows the pulse energy as a function of incident pump power. A 5 mJ pulse energy is obtained at maximum pump power with a pulse duration of 40 ns, as is shown in Fig. 8. The corresponding peak power is 125 kW.

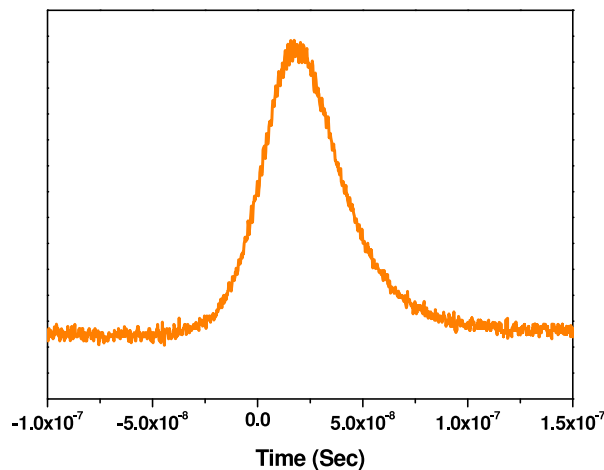


Fig. 8. Pulse profile of 1 kHz 1053 nm laser.

4. Conclusions

In summary, for end-pump configuration the pump position is also important in addition to the mode matching. We have developed a

model to calculate the optimal pump position so as to achieve best laser performance. Strategies to reduce the stress fracture of Nd:YLF is also considered in the laser design. Eventually, we have demonstrated a high energy high efficiency Nd:YLF laser operating at 1053 nm wavelength. For cw operation a 13.5 W output power is obtained with a slope efficiency of 51% and the beam quality is near diffraction limited with $M^2 \sim 1.02$. Under 1 kHz Q-switch operation, a high pulse energy of 5 mJ is obtained with a peak power of 125 kW. The attractive properties of Nd:YLF provide the considerable scope in high energy high beam quality lasers.

Acknowledgments

This work is supported by Advanced Optowave Corporation. Thanks to the laser scientists in the R&D department for valuable discussion.

References

- [1] T.M. Jeong, E.C. Kang, C.H. Nam, Temporal and spectral characteristics of an additive-pulse mode-locked Nd:YLF laser with Michelson-type configuration, *Opt. Commun.* 166 (1999) 95–102.
- [2] Mingjian Wang, Liang Zhu, Weibiao Chen, Dianyuan Fan, High-energy directly diode-pumped Q-switched 1617 nm Er:YAG laser at room temperature, *Opt. Lett.* 37 (2012) 3732–3734.
- [3] Tamer Kashef, Samy Ghoniemy, Ayman Mokhtar, Robust modeling and performance analysis of high-power diode side-pumped solid-state laser systems, *Appl. Opt.* 54 (2015) 10666–10677.
- [4] Qing-Lei Ma, Yong Bo, Nan Zong, Yu-Bai Pan, Qin-Jun Peng, Da-Fu Cui, Zu-Yan Xu, Light scattering and 2- μ m laser performance of Tm:YAG ceramic, *Opt. Commun.* 284 (2011) 1645–1647.
- [5] R. Biswas, A.S. Kuar, S. Sarkar, S. Mitra, A parametric study of pulsed Nd:YAG laser micro-drilling of gamma-titanium aluminide, *Opt. Laser Technol.* 42 (2010) 23–31.
- [6] Yang Pu, Lingyan Shi, Sebastiao Pratavieira, R.R. Alfano, Two-photon excitation microscopy using the second singlet state of fluorescent agents within the “tissue optical window”, *J. Appl. Phys.* 114 (2013) 153102.
- [7] M. Armstrong, X. Zhu, S. Gracewski, R.J.D. Miller, Development of a 25 W TEM₀₀ diode-pumped Nd:YLF laser, *Opt. Commun.* 169 (1999) 141–148.
- [8] Nan Zong, Qian-jin Cui, Qing-lei Ma, Xiao-fu Zhang, Yuan-fu Lu, Cheng-ming Li, Da-fu Cui, Zu-yan Xu, Huai-jin Zhang, Ji-yang Wang, High average power 1.5 μ m eye-safe Raman shifting in BaWO₄ crystals, *Appl. Opt.* 48 (2009) 7–10.
- [9] Y.J. Huang, C.Y. Tang, W.L. Lee, et al., Efficient passively Q-switched Nd:YLF TEM₀₀ mode laser at 1053 nm: selection of polarization with birefringence, *Appl. Phys. B* 108 (2012) 313–317.
- [10] Z. Zhang, Q. Liu, M. Nie, et al., Experimental and theoretical study of the weak and asymmetrical thermal lens effect of Nd:YLF crystal for σ and π polarizations, *Appl. Phys. B* 120 (2015) 689–696.
- [11] W.A. Clarkson, P.J. Hardman, D.C. Hanna, High-power diode-bar end-pumped Nd:YLF laser at 1.053 μ m, *Opt. Lett.* 23 (1998) 1363–1365.
- [12] Shan Xu, Shufang Gao, A new wavelength laser at 1370 nm generated by Nd:YLF crystal, *Mater. Lett.* 183 (2016) 451–453.
- [13] S. Xu, Y. Wei, C.H. Huang, W.D. Chen, F.J. Zhuang, L.X. Huang, G. Zhang, Efficient end-pumped Q-switched 1053 nm Nd:YLF laser with a plane-parallel resonator, *Opt. Commun.* 285 (2012) 1387–1389.
- [14] Christoph Bollig, Cobus Jacobs, M.J. Daniel Esser, Edward H. Bernhardt, Hubertus M. von Bergmann, Power and energy scaling of a diode-end-pumped Nd:YLF laser through gain optimization, *Opt. Express* 18 (2010) 13993–14003.
- [15] Y. Louyer, F. Balembois, M.D. Plimmer, T. Badr, P. Georges, P. Juncar, M.E. Himbert, Efficient cw operation of diode-pumped Nd:YLF lasers at 1312.0 and 1322.6 nm for a silver atom optical clock, *Opt. Commun.* 217 (2003) 357–362.
- [16] Y.F. Chen, T.S. Liao, C.F. Kao, T.M. Huang, K.H. Lin, S.C. Wang, Optimization of fiber-coupled laser-diode end-pumped lasers: influence of pump-beam quality, *IEEE J. Quantum Electron.* 32 (1996) 2010–2016.
- [17] Y.F. Chen, T.M. Huang, C.F. Kao, C.L. Wang, S.C. Wang, Optimization in scaling fiber-coupled laser-diode end-pumped lasers to higher power: influence of thermal effect, *IEEE J. Quantum Electron.* 33 (1997) 1424–1429.
- [18] Y.F. Chen, Design criteria for concentration optimization in scaling diode end-pumped lasers to high powers: influence of thermal fracture, *IEEE J. Quantum Electron.* 35 (1999) 234–239.
- [19] P.J. Hardman, W.A. Clarkson, G.J. Friel, M. Pollnau, D.C. Hanna, Energy-transfer upconversion and thermal lensing in high-power end-pumped Nd:YLF laser crystals, *IEEE J. Quantum Electron.* 35 (1999) 647–655.
- [20] Orazio Svelto, *Principles of Lasers*, Springer, 2010.
- [21] Qing-Lei Ma, Yong Bo, Nan Zong, Qin-Jun Peng, Da-Fu Cui, Yu-Bai Pan, Zu-Yan Xu, 108 W Nd: YAG ceramic laser with birefringence compensation resonator, *Opt. Commun.* 283 (2010) 5183–5186.
- [22] H. Kogelnik, T. Li, Laser beams and resonators, *Appl. Opt.* 5 (1966) 1550–1567.